American Mineralogist, Volume 59, pages 518–528, 1974

The Physical Properties of the Mg-Fe Richterites

ROBERT W. CHARLES
University of British Columbia,
Vancouver 8, British Columbia, Canada

Abstract

Six compositions of amphiboles along the join $Na_2CaMg_5Si_8O_{22}(OH)_2$–$Na_2CaFe_5Si_8O_{22}(OH)_2$ have been synthesized, and the physical properties studied with respect to P_{total}, T, and f_{O_2}. The f_{O_2} was controlled by standard oxygen buffering techniques. The unit cell data for the compositions studied on the iron-wüstite buffer are:

Composition	a(Å)	b(Å)	c(Å)	β	V(Å^3)
Mg_5	9.902(1)*	17.980(4)	5.269(1)	104°13(1)′	909.4(3)
Mg_4Fe_1	9.917(2)	18.020(5)	5.277(1)	104° 8(3)′	914.5(3)
Mg_3Fe_2	9.935(4)	18.063(3)	5.284(2)	104° 5(3)′	919.6(6)
Mg_2Fe_3	9.962(5)	18.122(6)	5.292(2)	104° 4(2)′	926.7(3)
Mg_1Fe_4	9.980(7)	18.180(7)	5.297(5)	103°58(2)′	932.7(9)
Fe_5	9.982(7)	18.223(6)	5.298(5)	103°44(7)′	936.2(1.0)

* *Parenthesized figures represent the estimated standard deviation (esd) in terms of least units cited for the value to their immediate left, thus 9.902(1) indicates an esd of 0.001.*

Refractive indices increase linearly from $\alpha = 1.604(5)$ and $\gamma = 1.622(3)$ at Mg_5 to $\alpha = 1.690(5)$ and $\gamma = 1.710(4)$ at Fe_5. Experiments on buffers above iron-wüstite (I-W) yielded large amounts of clinopyroxene in addition to amphibole.

Mössbauer studies indicate Fe^{3+} is present in all cases. This fact is explained by structural and local charge balance considerations. It is concluded that Na in the $M(4)$ site produces a local charge imbalance, which is corrected by placing Fe^{3+} in the neighboring $M(2)$ site. Na is lost from the A site to maintain charge balance.

Introduction

Richterites are monoclinic amphiboles having high sodium, moderate calcium, and low alumina contents and lying between the calcic and sodic amphiboles of Ernst (1968). The ideal formula is

$$Na_2Ca(Fe, Mg)_5Si_8O_{22}(OH)_2,$$

but substitutions of K^+ for Na^+ and F^- for OH^- are common in nature. The amphibole structure consists of double chains of silicon tetrahedra linked by the $M(1)$, $M(2)$, and $M(3)$ octahedra of 6-fold coordination and by the larger, 6- to 8-fold $M(4)$ sites (Papike, Ross, and Clarke, 1969). The still larger, 8- to 12-fold A site completes this linking strip of cations. In richterite the A site is 8-fold and contains Na, whereas the $M(4)$ site, also 8-fold, contains equal amounts of Na and Ca. The Fe and Mg are distributed between the remaining M sites, and OH^- occupies the O(3) sites.

Richterite is an uncommon alkali amphibole but is found in varied environments. Occurrences range from alkaline and peralkaline basalts to gneisses and impure metamorphosed limestones and meteorites. Analyses compiled by Deer, Howie, and Zussman (1963, pp. 352–358) indicate that most natural samples are relatively iron-free, or, when containing iron, much of it is in the ferric state. Richteritic amphibole has also been reported in an iron meteorite (Olsen, 1967) and in an enstatite chondrite (Douglas and Plant, 1968). Both of these examples contain significant amounts of F^- replacing OH^-.

Natural examples of ferrous richterites, though few in number, are known. The lunar basalts have yielded one richterite of composition

$$(K_{0.28}Na_{2.47}Ca_{0.33})(Mg_{3.57}Fe_{1.50}Al_{0.12})(Si_{7.99}Al_{0.01})O_{22}(OH, F)_2$$

(Gay, Bancroft, and Bown, 1970). All Fe was assumed

to be ferrous. Compared with the fluororichterite synthesized by Huebner and Papike (1970) and the hydrous ferrous richterites presented here, the fluorine content of the lunar amphibole was probably high. Ferrorichterite has been reported by Nicholls and Carmichael (1969) from a Kenya pantellerite, both in phenocrysts,

$$(K_{0.28}Na_{1.82}Ca_{0.77})(Fe_{4.68}Ti_{0.20}Mn_{0.13}Mg_{0.23})(Si_{7.78}Al_{0.11})O_{22}(OH_{1.39}F_{0.61}),$$

and as microlites in the glass,

$$(K_{0.31}Na_{2.02}Ca_{0.70})(Fe_{4.75}Ti_{0.19}Mn_{0.13}Mg_{0.17})(Si_{7.75}Al_{0.11})O_{22}(OH_{1.38}F_{0.62}).$$

Previous Investigations

Experimental work has been confined primarily to the magnesian end member. The fluorine analogue was first synthesized by Eitel (1954) and Comeforo and Kohn (1955), whereas hydrous richterite was synthesized by Phillips and Rowbotham (1968). Heubner and Papike (1970) studied the effect of potassium substitution in richterite, and the stability field of richterite was first defined by Forbes (1971).

Work on the ferrous compositions has been limited to a study of the stability of the hydrous analogue of a lunar richterite (Charles, Hewitt, and Wones, 1971), the synthesis of a potassic ferrorichterite by Huebner and Papike (1970), and the synthesis of a fluoro iron-bearing richterite by Cameron and Gibbs (1971). In Table 1 the cell parameters obtained by previous investigators are compared with the results of this study.

The molecule $Na_2Mg_6Si_8O_{22}(OH)_2$, "magnesiorichterite," was first prepared by Iiyama (1963); and Gibbs, Miller, and Shell (1962) determined the cell constants of its fluorine analogue. In this study magnesiorichterite refers to the composition $Na_2CaMg_5Si_8O_{22}(OH)_2$ and should not be confused with the calcium-free compositions.

Experimental Procedure

Oxide mixes were prepared for six compositions at equally spaced points on the join

$$Na_2CaMg_5Si_8O_{22}(OH)_2–Na_2CaFe_5Si_8O_{22}(OH)_2.$$

Iron was introduced as hematite, and portions of each mix were heated under H_2 to reduce the iron to the native state. Results were consistent regardless of the initial oxidation state of the iron. Oxygen fugacities were buffered using the following techniques: (1) solid oxygen buffers (Eugster, 1957); (2) hydrogen diffusion membrane (Shaw, 1967); (3) graphite-methane buffer (Eugster and Skippen, 1967). The charges and buffers were sealed in precious metal capsules and subjected to pressure and temperature in standard hydrothermal apparatus.

TABLE 1. Compositions and Cell Parameters of Synthetic Richterites

Reference	a (Å)	b (Å)	c (Å)	β	V (Å^3)
			$Na_2CaMg_5Si_8O_{22}(OH)_2$		
Phillips and Rowbotham (1968)*	9.902(2)**	17.980(4)	5.269(1)	104°12.7(1.1)'	909.4(3)
Huebner and Papike (1970)	9.907(2)	17.979(4)	5.269(1)	104°15.1(9)'	909.6(4)
Forbes (1971)	9.909(1)	17.978(5)	5.268(1)	104°13(2)'	909.9(2)
This study	9.902(2)	17.980(3)	5.269(1)	104°13(1)'	909.3(3)
			$KNaCaFe_5Si_8O_{22}(OH)_2$ (C-CH_4 Buffer)		
Huebner and Papike (1970)	10.172(3)	18.201(7)	5.290(2)	104°32(2)'	948.2(4)
			$Na_2CaFe_5Si_8O_{22}(OH)_2$ (I-W Buffer)		
This study	9.982(7)	18.223(6)	5.298(5)	103°44(7)'	936.2(1.0)
Calculated from Huebner and Papike (1970)					936.6

*Refinement of Huebner and Papike (1970).

**Parenthesized figures represent the estimated standard deviation (esd) in terms of least units cited for the value to their immediate left, thus 9.902(2) indicates an esd of 0.002.

Description of Phases

Microscopic examination reveals that 2-day experiments at 800°C and 1 kbar produced 98–100 percent magnesiorichterite. The amphibole consisted of elongate euhedral grains, some occurring in a felty mass. Amphibole containing iron was grown most readily on the iron-wüstite (I-W) buffer. Compositions containing more iron than Fe_2Mg_3 invariably produced 20–30 percent clinopyroxene in addition to amphibole on buffers more oxidizing than iron-wüstite. At more oxidizing buffers than C-CH_4 only the $FeMg_4$ composition could be grown at greater than 95 percent purity. However, even $FeMg_4$ yielded significant amounts of clinopyroxene (>10 percent) on the hematite-magnetite (H-Mt) buffer. High purity is important because the pyroxene grown on H-Mt is acmitic, judging from the powder X-ray diffraction pattern. If the clinopyroxene exceeds a

few percent, the resulting amphibole is nonstoichiometric, as shown by the lattice parameters for Mg_4Fe on various buffers. Small amounts (<5 percent) of pyroxene, olivine, and glass were assumed to be roughly equal to the bulk composition of the mix. For such a small amount of pyroxene the partitioning of Fe and Mg between pyroxene and amphibole was ignored. The effect of the introduction of pyroxene to the products is shown in Figure 1 and Table 2 for results on quartz-fayalite-magnetite (QFM). Between Mg_4Fe and Mg_3Fe_2 pyroxene appears, and on Mg_3Fe_2 equals about 10–15 percent of the products. The cell volume for Mg_3Fe_2 approximately equals that for Mg_4Fe. Pyroxene increases in abundance until 30–40 percent of the charge is pyroxene at Fe_5. Attempts to produce ferrorichterite on the QFM buffer yielded a very dark green amphibole plus about 40 percent pyroxene. Presumably, the color indicates the increased content of ferric iron in the amphibole.

The amphibole changed greatly in optical character along the magnesiorichterite-ferrorichterite join. Figure 2 and Table 3 display the change in refractive indices on the I-W buffer. The extinction angle ($\gamma \wedge Z$) increases from roughly 5°–10° for the magnesian compositions to 10°–15° for the iron-rich varieties. Color varies from white to green across the compositional field. The pleochroism—*X*-green; *Y*-yellow-green; *Z*-green—is most easily seen in the more ferrous amphiboles.

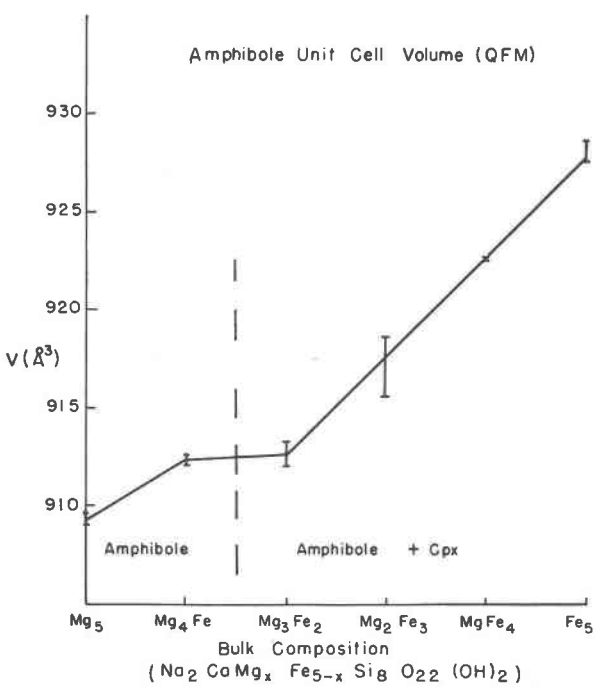

FIG. 1. Cell volume *vs* composition for amphibole grown on the QFM buffer at various pressures and temperatures.

Experiments conducted on I-W at low temperatures (500°–550°C) produced a finely crystalline mass containing >95 percent amphibole with subordinate pyroxene, olivine, and clear glass for the compositions Mg_4Fe through Mg_2Fe_3. Most of the crystals, regardless of composition, were <5 μm in greatest dimension. The $MgFe_4$ richterite was difficult to grow at less than 5 kbar. Almost invariably, charges of this composition contained >10 percent pyroxene at low pressures. The $MgFe_4$ amphibole was always very hard and brittle whereas all other compositions were soft and fibrous.

Ferrorichterite can be characterized as a short prismatic green amphibole with $n\alpha = 1.710(3)$ and $n\gamma = 1.690(5)$. Two varieties were synthesized. Shorter synthesis experiments (<10 days) at higher temperatures (600°–700°C) resulted in a coarse amphibole accompanied by about 10 percent clinopyroxene, fayalite, and a trace of glass. Longer experiments (22–30 days) at lower temperatures (500°–530°C) yielded fine-grained amphibole (>95 percent) plus a few percent clinopyroxene, olivine, and clear glass. The pyroxene was a striking bright green with refractive index around 1.730. Fayalite appeared as roughly equant grains with a light brown color. It is important to point out that less ferrous compositions yielded only one variety of amphibole regardless of the synthesis time.

For the series in general, clinopyroxene, olivine, and glass were always less than 5 percent for compositions Mg_5 through Mg_2Fe_3 and for long experiments on Fe_5. Short experiments on Fe_5 and low-pressure experiments on $MgFe_4$ (<5 kbar) yielded 10 percent or more clinopyroxene, olivine, and glass. Long experiments on Fe_5 contained more glass than those on any other bulk composition; however, the amount was only 2–3 percent.

X-Ray Determinations

The unit cell parameters were determined using a Norelco powder X-ray diffraction goniometer. Scans of 1/2° per minute at a strip chart recorder rate of 1/2 in. per minute were satisfactory to fix the peak positions of amphibole to ±0.01°, standardized against BaF_2 ($a = 6.1971 \pm 0.0002$ Å). BaF_2 in turn was standardized against diamond ($a = 3.56703 \pm 0.00018$ Å) and has four usable reflections between 24° and 49°. The 220 reflection of BaF_2 at 41.164°

TABLE 2. Cell Parameters

Composition	T (°C)	P (kbar)	Duration (hr)	a (Å)	b (Å)	c (Å)	β	V (Å^3)	a sin β (Å)
$Na_2CaMg_5Si_8O_{22}(OH)_2$	850	1	48	9.903(1)*	17.982(2)	5.267(1)	104°14'(1')	909.2(1)	
"	850	1	96	9.903(3)	17.976(4)	5.270(2)	104°13'(1')	909.4(3)	
"	800	1	48	9.901(2)	17.976(4)	5.270(1)	104°12'(1')	909.3(3)	
"	800	1	96	9.901(2)	17.987(2)	5.270(1)	104°12'(1')	909.9(4)	
Ave.				9.902(1)	17.980(4)	5.269(1)	104°13'(1')	909.4(3)	9.599(1)
				Fe_3O_4-Fe_2O_3 Buffer					
"$Na_2CaFeMg_4Si_8O_{22}(OH)_2$" + Px	800	1	72	9.839(4)	17.963(7)	5.276(2)	104°2'(2')	904.6(4)	
" "	800	1	96	9.835(5)	17.978(6)	5.282(2)	104°4'(2')	906.0(4)	
" "	650	1	288	9.823(5)	17.964(6)	5.285(3)	103°59'(2')	905.0(4)	
" "	650	1	,240	9.838(3)	17.944(6)	5.281(2)	103°56'(2')	904.9(4)	
Ave.				9.834(6)	17.962(10)	5.281(3)	104°0'(3')	905.1(5)	9.542(6)
				Ni-NiO Buffer					
$Na_2CaFeMg_4Si_8O_{22}(OH)_2$	800	1	96	9.898(3)	18.019(7)	5.279(3)	104°7'(3')	913.1(5)	
"	800	1	96	9.894(2)	18.004(3)	5.279(2)	104°3'(1')	912.0(4)	
"	800	1	72	9.901(1)	18.003(4)	5.278(1)	104°5'(1')	912.5(2)	
"	650	1	240	9.894(3)	18.005(8)	5.275(2)	104°5'(3')	911.5(5)	
Ave.				9.898(4)	18.009(7)	5.277(2)	104°5'(2')	912.4(6)	9.601(4)
				Fe_2SiO_4-SiO_2-Fe_3O_4 Buffer					
$Na_2CaFeMg_4Si_8O_{22}(OH)_2$	800	1	72	9.896(2)	18.003(4)	5.279(2)	104°5'(1')	912.3(3)	
"	800	1	144	9.890(2)	18.003(6)	5.282(1)	104°4'(1')	912.2(3)	
"	650	1	240	9.891(4)	18.000(13)	5.283(2)	104°3'(2')	912.4(4)	
"	600	7	96	9.891(8)	18.013(5)	5.285(4)	104°10'(4')	912.9(8)	
Ave.				9.892(2)	18.005(5)	5.282(2)	104°6'(3')	912.4(3)	9.593(2)
				C-CH_4 Buffer					
$Na_2CaFeMg_4Si_8O_{22}(OH)_2$	650	1	240	9.904(4)	18.017(3)	5.276(1)	104°10'(3')	912.8(4)	
"	650	1	144	9.906(4)	17.995(6)	5.278(2)	104°9'(3')	912.3(5)	
"	650	1	288	9.904(3)	18.000(4)	5.279(1)	104°6'(1')	912.7(3)	
Ave.				9.905(2)	18.004(9)	5.278(1)	104°8'(2')	912.7(2)	9.605(2)
	800	1	72	9.902(3)	18.017(4)	5.276(1)	104°6'(1')	912.9(2)	
				Fe-FeO Buffer					
$Na_2CaFeMg_4Si_8O_{22}(OH)_2$	650	1	144	9.916(2)	18.017(4)	5.276(1)	104°4'(1')	914.8(2)	
"	650	1	144	9.913(4)	18.017(7)	5.277(2)	104°4'(3')	914.2(4)	
"	650	1	168	9.918(3)	18.019(5)	5.277(2)	104°10'(2')	914.4(4)	
"	650	2	96	9.919(4)	18.022(6)	5.276(2)	104°10'(2')	914.4(4)	
"	600	7	120	9.917(2)	18.027(4)	5.276(1)	104°10'(1')	914.6(2)	
"	550	5	96	9.916(4)	18.024(4)	5.280(1)	104°8'(2')	915.0(3)	
"	530	10	312	9.918(6)	18.015(9)	5.277(3)	104°9'(4')	914.3(5)	
Ave.				9.917(2)	18.020(5)	5.277(1)	104°8'(3')	914.5(3)	9.617(2)
$Na_2CaFe_2Mg_3Si_8O_{22}(OH)_2$	650	1	144	9.936(4)	18.062(7)	5.285(2)	104°4'(3')	920.0(4)	
"	650	1	144	9.930(4)	18.064(6)	5.283(3)	104°3'(2')	919.3(4)	
"	650	1	168	9.936(4)	18.065(6)	5.287(2)	104°4'(2')	920.5(4)	
"	650	2	144	9.935(4)	18.057(6)	5.279(2)	104°6'(2')	918.5(4)	
"	600	7	120	9.938(2)	18.067(3)	5.284(1)	104°10'(3')	920.0(2)	
"	550	5	198	9.942(5)	18.089(11)	5.287(3)	104°9'(3')	921.9(7)	
"	530	10	333	9.927(5)	18.064(8)	5.285(2)	104°5'(2')	919.2(5)	
Ave.				9.935(4)	18.063(3)	5.284(2)	104°5'(3')	919.6(6)	9.636(4)
$Na_2CaFe_3Mg_2Si_8O_{22}(OH)_2$	600	7	120	9.970(4)	18.126(5)	5.289(1)	104°6'(2')	927.0(4)	
"	530	2	599	9.955(3)	18.130(5)	5.293(1)	104°0'(1')	926.9(3)	
"	530	5	547	9.962(4)	18.122(6)	5.294(2)	104°4'(3')	927.6(4)	
"	530	10	595	9.958(9)	18.113(11)	5.293(3)	104°4'(5')	926.1(7)	
"	500	2	480	9.964(3)	18.121(4)	5.291(1)	104°5'(1')	926.6(3)	
Ave.				9.962(5)	18.122(6)	5.292(2)	104°4'(2')	926.7(3)	9.663(5)
$Na_2CaFe_4MgSi_8O_{22}(OH)_2$	700	5	240	9.980(4)	18.185(6)	5.300(1)	103°56'(1')	933.6(4)	
"	600	7	120	9.988(2)	18.184(4)	5.292(1)	103°57'(2')	932.8(2)	
"	530	10	962	9.973(3)	18.172(5)	5.301(1)	104°0'(2')	931.8(3)	
Ave.				9.980(7)	18.180(7)	5.297(5)	103°58'(2')	932.7(9)	9.685(5)
I. $Na_2CaFe_5Si_8O_{22}(OH)_2$ + Px	600	7	120	10.002(4)	18.232(7)	5.307(2)	103°56'(2')	939.4(5)	
"	700	5	216	10.003(5)	18.245(7)	5.309(2)	103°56'(2')	940.4(5)	
Ave.				10.003(1)	18.238(8)	5.308(1)	103°55'(1')	940.0(7)	9.710(1)
II. $Na_2CaFe_5Si_8O_{22}(OH)_2$	530	10	535	9.975(2)	18.226(6)	5.292(2)	103°37'(8')	935.0(5)	
"	530	5	721	9.990(3)	18.216(6)	5.303(2)	103°51'(2')	937.0(4)	
"	500	2	672	9.980(8)	18.227(6)	5.300(6)	103°44'(5')	936.5(6)	
Ave.				9.982(7)	18.223(6)	5.298(5)	103°44'(7')	936.2(1.0)	9.697(6)

*Parenthesized figures represent the estimated standard deviation (esd) in terms of least units cited for the value to their immediate left, thus 9.903(1) indicates an esd of 0.001.

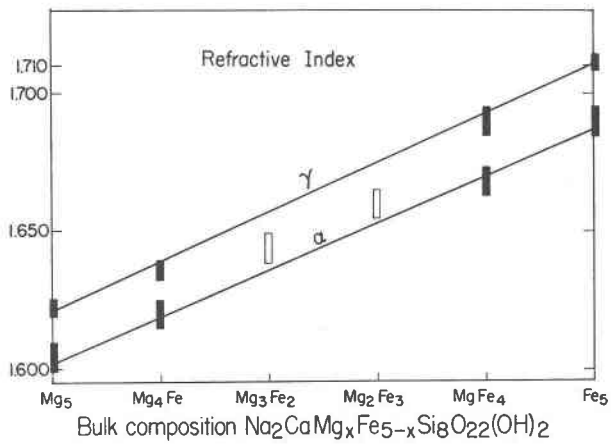

FIG. 2. Alpha and gamma refractive indices for the amphibole series grown on the I-W buffer. Mg_3Fe_2 and Mg_2Fe_3 yielded only bulk indices.

could not be used for compositions more iron-rich than Mg_3Fe_2 owing to overlap of the 261 reflection of the richterites. The richterites were indexed and cell parameters calculated using a program developed by Evans, Appleman, and Handwerker (1963). Twenty-four reflections for magnesiorichterite were unambiguously indexed using the cell refinements of Huebner and Papike (1970). The number of usable reflections decreases to sixteen for ferrorichterite. Some peaks, for example 020, decrease in intensity; others are broadened by poorer crystallinity; and one, 261, interferes with a standard peak.

A continuous shift in peak position toward lower angles and changes in intensity of a given reflection occur with addition of iron. Sample results are reproduced in Table 4 for magnesiorichterite and ferrorichterite. All cell dimension data with buffer and *P-T* conditions are listed in Table 2.

TABLE 3. Optical Properties

Composition ($Na_2CaMg_4Fe_{5-x}Si_8O_{22}(OH)_2$)	Buffer	α	γ	Mean R.I.	Maximum Size (μm)
Mg_5	...	1.604(5)*	1.622(3)	...	35 x 5
Mg_4Fe	I-W	1.620(5)	1.636(3)	...	15 x 3
"	C-CH_4	...	...	1.632(5)	< 5
"	QFM	1.620(5)	1.636(3)	...	25 x 5
"	N-NO	...	...	1.632(5)	7 x 1
"	H-Mt	1.616(5)	1.630(3)	...	10 x 2
Mg_3Fe_2	I-W	...	...	1.644(5)	5 x 1
Mg_2Fe_3	I-W	...	...	1.660(5)	5 x 1
$MgFe_4$	I-W	1.668(5)	1.680(5)	...	30 x 10
Fe_5	I-W	1.690(5)	1.710(4)	...	10 x 2

*Parenthesized figures represent the estimated standard deviation (esd) in terms of least units cited for the value to their immediate left, thus 1.604(5) indicates an esd of 0.005.

The uniformity of cell parameters on I-W in *P-T* space is shown in Figure 3 for Mg_4Fe, Mg_3Fe_2, and Mg_2Fe_3. The cell volumes of quench phases remain essentially constant in the pressure range 1 to 10 kbar and temperature range 500° to 650°C.

Mg-richterite has a rather low stability limit with respect to pressure, as indicated by the experiments listed in Table 5. Changes in cell dimensions occurred between 2 and 7 kbar even though the charge was >95 percent amphibole. Experiments of 6 days at 7 kbar and 600°C using an oxide mix yielded quartz in addition to amphibole. Quartz is gradually resorbed and after 20 days is absent. At 10 kbar and 510°C, experiments of 25 days' duration produced persistent quartz plus an amphibole with a powder pattern not unlike that of tremolite. The cell parameters do show some trend toward tremolite with increasing *P*. Most striking is the distinct trend of $a \sin \beta$ and b.

Addition of Fe to richterite apparently stabilized the structure to higher *P* because all experiments at high *P* containing iron show no variation in cell parameters. Greater iron concentrations (*i.e.*, $MgFe_4$ and Fe_5) were not plotted because the number of experiments is insufficient to show any trend in cell volume with *P* and *T*.

The uniformity of cell volume on a given buffer is shown in Figure 4 for Mg_4Fe at a P_{total} of 1 kbar. Two points should be noted here. First, the uniformity of the amphibole cell volume even in the presence of large amounts (>10 percent) of pyroxene on H-Mt is evident. [The pyroxene will be completely characterized in a later paper on a study of the phase equilibria of the richterites. Preliminary examination of its cell constants indicates it is an acmitic diopside.] Second, the apparent constancy of the cell volume along the C-CH_4 buffer is unexpected. Because the C-CH_4 buffer does not parallel the other buffer curves, the volume should increase at higher temperatures. This effect, however, is not recognized for so small a concentration of iron. Other compositions of amphibole on buffer curves more oxidizing than I-W will be examined closely in the phase equilibrium studies for uniformity with *P* and *T*.

Figure 5 exhibits the variation in cell volume and $a \sin \beta$ with oxygen fugacity at $P_{total} = 1$ kbar, $T = 650$°C, and constant composition (Mg_4Fe). Cell volume and $a \sin \beta$ are largest for the iron-wüstite (I-W) buffer but are roughly equal for fugacities

TABLE 4. X-Ray Powder Reflections of End Members Richterite and Ferrorichterite

hkl	$Na_2CaMg_5Si_8O_{22}(OH)_2$					$Na_2CaFe_5Si_8O_{22}(OH)_2$				
	d_{hkl}		2θ		I/I_o	d_{hkl}		2θ		I/I_o
	obs.	calc.	obs.	calc.		obs.	calc.	obs.	calc.	
020	8.9908	8.9928	9.829	9.827	10	...	9.1079	...	9.703	...
110	8.4682	8.4701	10.437	10.435	40	8.5767	8.5614	10.323	10.323	100
-111	4.8637	4.8603	18.224	18.237	20	...	4.8925	...	18.116	...
200	4.7997	4.7977	18.469	18.477	15	4.8522	4.8498	18.268	18.277	10
040	4.4954	4.4953	19.732	19.732	30	4.5582	4.5540	19.457	19.476	20
111	4.0053	4.0067	22.175	22.167	15	4.0542	4.0506	21.904	21.924	5
-131	3.8629	3.8615	23.003	23.012	30	3.8964	3.8958	22.796	22.806	10
131	3.3888	3.3899	26.275	26.267	65	3.4287	3.4288	25.964	25.964	35
240	3.2810	3.2801	27.155	27.163	45	3.3183	3.3198	26.844	26.832	25
310	3.1503	3.1514	28.305	28.295	90	3.1841	3.1834	27.998	28.004	65
221	2.9591	2.9588	30.175	30.179	60	2.9962	2.9953	29.793	29.803	25
-151	2.9298	2.9297	30.485	30.486	15	...	2.9604	...	30.162	...
330	2.8228	2.8217	31.670	31.683	25	2.8525	2.8538	31.332	31.317	15
-331	2.7341	2.7346	32.725	32.720	20	...	2.7550	...	32.470	...
151	2.7061	2.7056	33.075	33.068	100	2.7386	2.7392	32.670	32.663	70
061	2.5846	2.5859	34.677	34.673	45	2.6154	2.6152	34.256	34.258	35
-202	2.5260	2.5260	35.508	35.508	65	2.5396	2.5396	35.312	35.312	50
350	2.3905	2.3913	37.593	37.581	15	...	2.4182	...	37.147	...
-171	2.2898	2.2898	39.314	39.314	25	...	2.3160	...	38.851	...
-312	2.2703	2.2704	39.665	39.664	25	2.2823	2.2819	39.448	39.455	15
261	2.1659	2.1656	41.664	41.669	45	...	2.1932	...	41.122	...
202	2.0542	2.0546	44.043	44.034	25	2.0757	2.0773	43.565	43.579	10
351	2.0268	2.0265	44.627	44.679	15	2.0518	2.0520	44.099	44.093	20
510	1.9090	1.9091	47.593	47.596	15	...	1.9290	...	47.069	...
	(800°C, 1 kbar, 2 days)					(I-W, 530°C, 5 kbar, 30 days)				

between the C-CH_4 and nickel-nickel oxide (N-NO) buffers. At f_O, higher than the N-NO buffer, pyroxene appears in increasing amounts, causing the unit cell volume of the amphibole to drop off rapidly. The trend in lattice parameters is generally toward magnesioriebeckite.

Because the I-W buffer produced the highest yields of amphibole, the cell parameters calculated from these run products must be examined very closely to interpret the variations in these parameters in light of the richterite structure. The data plotted in Figure 6 are taken from Table 2. Both ferrorichteritic amphiboles are plotted, with experiments of lower yield plotted in parentheses. The parameters a, c, and $a \sin \beta$ increase almost linearly from Mg_5 to $MgFe_4$; for more iron-rich compositions, however, the curves for all parameters appear to branch. The values for b are slightly below the line for the compositions Mg_4Fe, Mg_3Fe_2, and Mg_2Fe_3, whereas β decreases monotonically. The volume of mixing for the compositions Mg_4Fe and Mg_3Fe_2 is slightly negative. Ideal mixing, of course, would be linear. Only some of these observations are statistically real. These observations and structural arguments will be applied to show that the less statistically accurate deviations from linearity are also real.

Each straight line and dashed extension in Figure 6

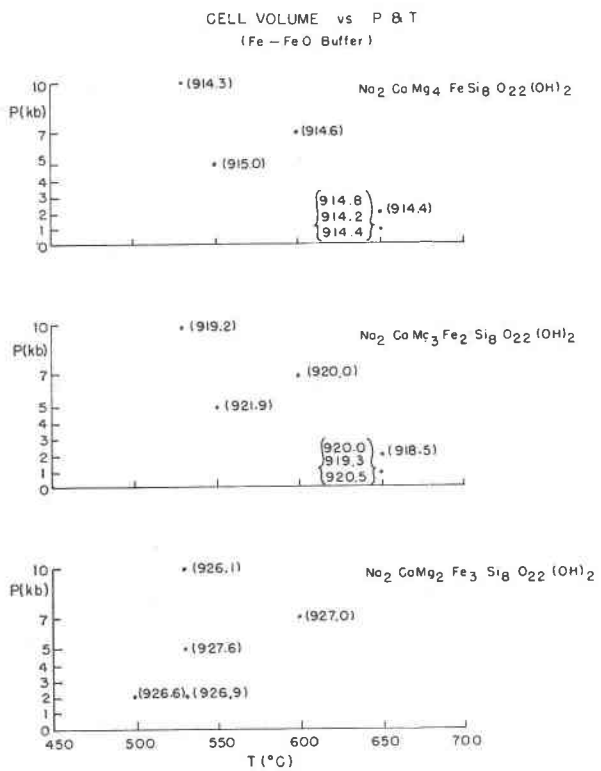

FIG. 3. Uniformity of unit cell volume throughout the P, T space investigated. Higher iron compositions were not plotted owing to fewer data points. Uniformity may not be true for Mg_5.

TABLE 5. Mg-Richterite at Increasing Pressure

P (bars)	T (°C)	Duration (hr)	a (Å)	b (Å)	c (Å)	β	V (Å^3)	a sin β (Å)
1000	700	72	9.901(2)*	17.976(4)	5.270(1)	104°12'(1')	909.4(0.3)	9.599
2000	800	48	9.903(1)	17.982(2)	5.267(1)	104°14'(1')	909.2(0.1)	9.599
5000	700	119	9.884(7)	17.984(7)	5.268(3)	104°4'(5')	907.7(0.6)	9.587
7000	600	456	9.893(3)	18.003(8)	5.268(2)	104°14'(2')	909.5(0.4)	9.589
10,000	510	600	9.896(7)	18.001(9)	5.270(3)	104°20'(3')	909.6(0.6)	9.588
Tremolite (Papike et al., 1969)			9.818(5)	18.047(8)	5.275(3)	104°39'(3')	904.2(0.6)	9.499

*Parenthesized figures represent the estimated standard deviation (esd) in terms of least units cited for the value to their immediate left, thus 9.901(2) indicates an esd of 0.002.

was drawn not as a least-squares fit but with these considerations in mind: (1) the Mg_5 composition yields correct parameters; (2) it is assumed that A and $M(4)$ are uniformly occupied by the same cations throughout, and all other M sites are the same size with no preferred ordering of cations. Obviously, (2) is not true and deviations from linearity will be discussed on such a basis.

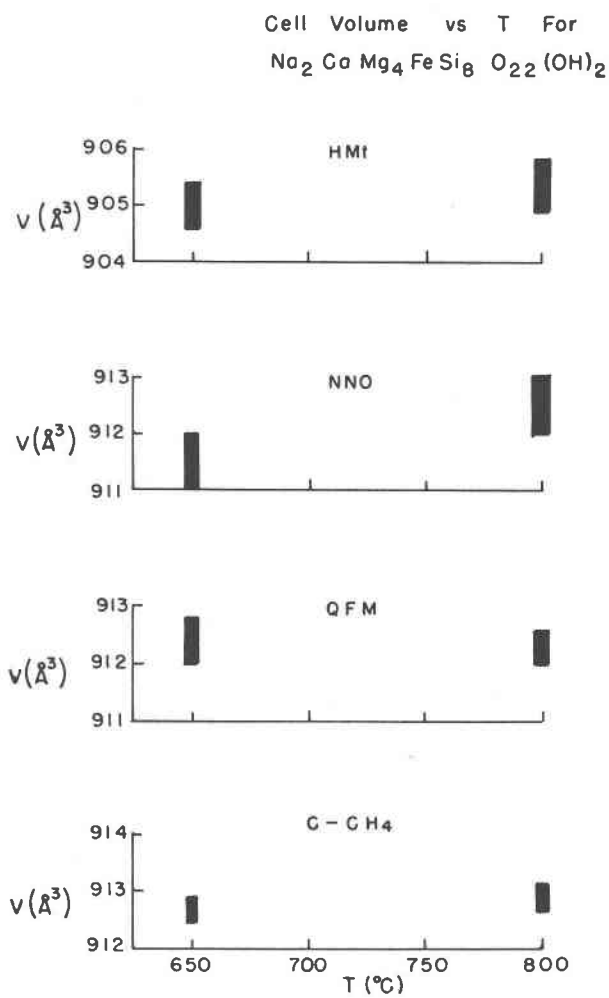

FIG. 4. Uniformity of cell volume along a given buffer for Mg_4Fe at P_{total} = 1 kbar.

Preliminary results from Mössbauer work by D. Virgo (personal communication, 1972) indicate roughly 5 percent ferric iron is present in the amphibole at Fe_5 that is on the linear trend shown in the cell parameter diagrams. The purest ferrorichterite, however, contains noticeably more (>10 percent) ferric iron and deviates from this trend. At least four mechanisms of incorporation of ferric iron into the amphibole structure relevant here are possible. First, ferric iron commonly can be explained by assuming that Fe^{3+} and O^{2-} replace Fe^{2+} and OH^- to produce oxyamphibole. Effectively, hydrogen is removed from the structure and iron is oxidized to Fe^{3+}. Second, H_2O may leach Na from the amphibole so that Fe^{3+} and a vacancy substitute for Fe^{2+} and Na. Third, either of these could be accomplished if there is a structural limitation on the amount of ferrous iron in the five $M(1)$, $M(2)$, and $M(3)$ sites in the unit cell. Bancroft and Burns (1969), Wilkins (1970), and Mitchell, Bloss, and Gibbs (1970) indicate that the $M(2)$ site is smaller in hydrous amphiboles and generally accepts magnesium or ferric iron instead of the larger ferrous iron. This may not be true for fluoroamphiboles (Cameron and Gibbs, 1971) because iron does not coordinate well with fluorine. The only M sites not coordinated with fluorine in O_3 are the two $M(2)$ sites. Fourth, Ghose (1966) and Whittaker (1949, 1960) postulated that, if Na occupies the $M(4)$ site, a local charge imbalance will result since the Na is coordinated with six oxygens. Such an imbalance would be corrected by addition of ferric iron into the $M(2)$ site because $M(2)$ lies closest to $M(4)$ (Papike, Ross, and Clarke, 1969).[1] To complete charge balance in richterites, either Na^+ or H^+ must

[1] For potassic richterite: $M(2)$–$M(4)$ = 3.182 Å; $M(1)$–$M(4)$ = 3.410 Å.

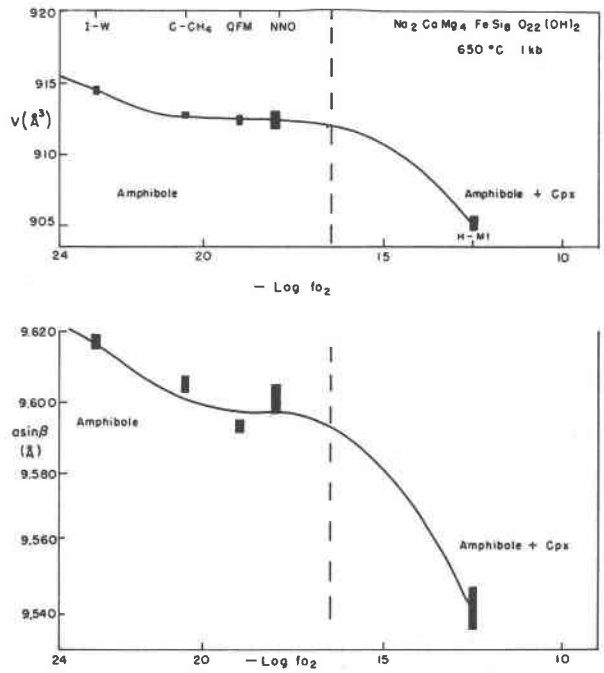

FIG. 5. Variation of cell volume with log f_{O_2} for Mg_4Fe at $T = 650°C$, $P_{total} = 1$ kbar.

be removed elsewhere. Burns and Prentice (1968) support the charge balance theory by reporting the preferential positioning of Fe^{3+} in $M(2)$ in riebeckites ($Na_2Fe^{2+}{}_3Fe^{3+}{}_2Si_8O_{22}(OH)_2$), which necessarily have Fe^{3+} in their structural formula.

Discussion

The key to the interpretation appears to be that (1) all experiments on I-W contain a trace amount of glass, and (2) the long syntheses of ferrorichterite (22–30 days) contain a larger amount of glass. Production of an oxyamphibole would yield no glass. The H_2O leaching of Na and Si should have caused more scatter in the data points depending upon time and the amount of H_2O in the experiments. In addition, leaching would not have preferentially occurred in long syntheses of just ferrorichterite composition. Syntheses of equal or longer duration were performed on Fe_3Mg_2 and Fe_4Mg with no such branching of the cell parameters. Any explanation such as alloying of iron in the $Ag_{80}Pd_{20}$ fails for the same reason. One is left with the conclusion that five ferrous irons may just be too large to fit in the amphibole structure, especially in close proximity to Na in $M(4)$. Because all experiments on I-W started with a reduced mix containing native iron, short experiments on this buffer may have metastably yielded a ferrous amphibole whose ferrorichterite composition agrees with the extrapolated cell parameter curves. This amphibole, presumably not the stable form, is more nearly a completely ferrous amphibole. Preliminary Mössbauer results indicate that the Fe^{3+}/Fe^{2+} ratio for this phase is less than that for Mg_2Fe_3.

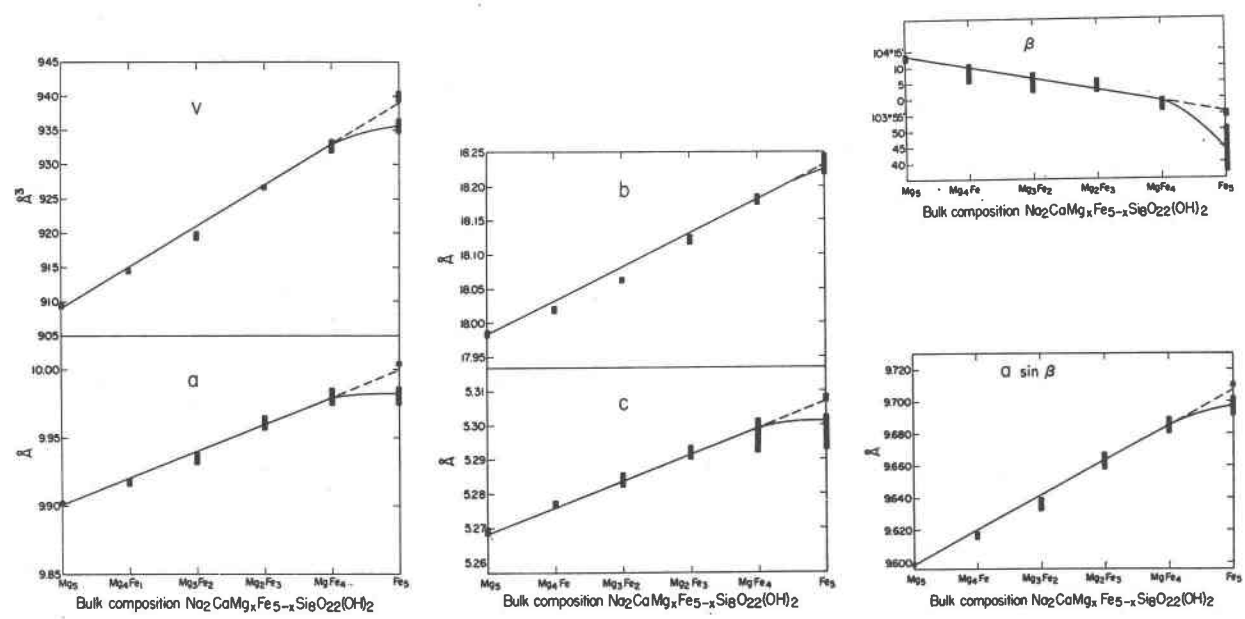

FIG. 6. Variation of unit cell parameters for the amphibole series grown on I-W. Both Fe_5 varieties are plotted.

Using these interpretations, the observed lattice constants can be explained completely. The parameter a depends upon the mean size of the cations in the linking cation strip (Ernst, 1968; Huebner and Papike, 1970). It should be a linear function if the incremental change in cation size remains constant as one proceeds across the series. Beyond $MgFe_4$, the mean size of the cations increases at a smaller rate because of sodium loss and the introduction of more ferric iron.

The parameter b is influenced most by the occupancy of the $M(4)$ and $M(2)$ sites, which actually link the double chains of silicon tetrahedra (Colville, Ernst, and Gilbert, 1966; Ernst, 1968). The $M(4)$ site is occupied by Na and Ca in all these amphiboles. Of secondary importance are the other M sites. Although not actually linking the double chains, they may cause some increase in the b dimension when occupied by larger cations. The diagram presented here clearly shows that, while the two $M(1)$ and $M(3)$ sites are filling preferentially with ferrous iron (Mg_4Fe to Mg_2Fe_3), the observed points drop below the line representing uniform, totally disordered filling of the M sites. Complete ordering is not observed from the Mössbauer spectra. More will be stated on this point when all the Mössbauer data are analyzed. The deviation at Fe_5 is small. Only 10 percent ferric iron apparently has little effect on the b dimension.

The parameter c, or chain length, is controlled by (1) the size of cations in the $M(1)$ and $M(3)$ sites (Colville, Ernst, and Gilbert, 1966) and/or (2) the size of the tetrahedral cations (Ernst, 1968). In spite of the great difference in size between Fe^{3+} and Si in 4-fold coordination, 0.40 Å *vs* 0.63 Å (Shannon and Prewitt, 1969), local charge imbalance may require some Fe^{3+} to enter and lengthen the chain to balance the Na in the A site. Judging from the structure, large cations in $M(2)$ should also affect the chain length. Once again an essentially uniform linear trend is observed until more ferric iron is present, causing a much smaller stretching of the chain. If the increased Fe^{3+} goes into $M(2)$ instead of a tetrahedral site, less expansion occurs along c, as is observed.

Huebner and Papike (1970) show clearly that the A site controls angle β as well as influencing a. Addition of larger cations to A causes β to increase. In sodic richterite the A is uniformly filled with Na, but as one proceeds from Mg_5 to Fe_5 the structure expands around the Na to produce an effect equivalent to placing a relatively smaller cation in the A site. Consequently, β decreases. Near Fe_5, it decreases more sharply owing to not only Fe^{3+} but actual Na loss.

The parameter $a \sin \beta$ reflects the mean size of the cations in the linking cation layer more clearly than does a because this dimension is perpendicular to the layer of M sites. The $M(1)$ sites project more into the rings formed by the double chains and have less influence than the other M sites. Also, a larger portion of the iron in lower iron compositions is Fe^{3+} owing to Na in $M(4)$. The effect is small, but it can be seen in the compositions Mg_4Fe and Mg_3Fe_2, which fall below the linear curve. Loss of Na and oxidation of Fe^{2+} cause a small decrease at Fe_5.

Combining the effects of all other cell parameters, the cell volume shows a slightly negative volume of mixing on the low-iron compositions and a slightly positive volume of mixing on the high-iron compositions.

Using these physical properties, ferrorichterite can be compared with the other iron-bearing amphiboles. The stability of ferropargasite ($NaCa_2Fe^{2+}{}_4AlSi_6Al_2O_{22}(OH)_2$), ferrotremolite ($Ca_2Fe_5Si_8O_{22}(OH)_2$), and riebeckite-arfvedsonite ($Na_{2.4}Fe^{2+}{}_{4.9}Fe^{3+}{}_{0.7}Si_{7.7}Fe^{3+}{}_{0.3}(OH)_2$) have been experimentally defined by Gilbert (1966), Ernst (1966), and Ernst (1962), respectively. Table 6 and Figure 7 show pertinent data regarding their upper stability limits. The decomposition curve of ferrorichterite has been added. Its phase equilibria will be covered in more detail in a later paper. When these results are compared, calcium *vs* sodium should have little effect on the stability limit (Ernst, 1968).

Ferropargasite, which shows the greatest stability, has Al and Fe^{2+} in the $M(2)$ sites and Al in the double chains. Ferropargasite is stable to a much higher f_{O_2}, owing principally to the lack of Na in $M(4)$. At lower f_{O_2} (QFI), this amphibole becomes less stable with respect to temperature because of the great decrease

TABLE 6. Ferrous Amphibole Stabilities on I-W Buffer

Phase and Composition	Stability Limit P (bars)	Stability Limit T (°C)	Reference
Ferrotremolite	500	437	Ernst (1966)
	1000	465	
$Ca_2Fe^{2+}{}_5Si_8O_{22}(OH)_2$	1500	485	
	2000	506	
Riebeckite-arfvedsonite	500	670	Ernst (1962)
	1000	690	
$Na_{2.4}Fe^{2+}{}_{4.9}Fe^{3+}{}_{0.7}Si_{7.7}Fe^{3+}{}_{0.3}O_{22}(OH)_2$	1500	700	
	2000	710	
Ferrorichterite	500	690	This study
	1000	715	
$Na_2CaFe^{2+}{}_5Si_8O_{22}(OH)_2$	1500	725	
	2000	735	
Ferropargasite	500	682	Gilbert (1966)
	1000	800	
$NaCa_2Fe^{2+}{}_4AlSi_8O_{22}(OH)_2$	1500	835	
	2000	850	

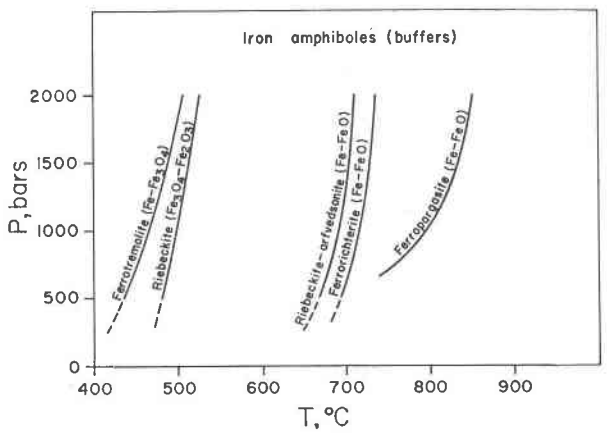

FIG. 7. Comparison of the thermal stability limits of ferrotremolite (Ernst, 1966), riebeckite (Ernst, 1962), riebeckite-arfvedsonite (Ernst, 1962), ferrorichterite (this paper), and ferropargasite (Gilbert, 1966). Oxygen fugacities are defined by the labeled buffer systems.

in activity of H_2O under these conditions, a factor unrelated to the ferrous-ferric problem.

Ferrotremolite has complete local charge balance. Consequently, five ferrous irons are placed into the five available *M* sites. The predicted increase in *b* for the conversion of tremolite to ferrotremolite is calculated as 0.32 Å (Colville, Ernst, and Gilbert, 1966). Colville *et al* experimentally observed an increase of 0.29 Å, which was considered within the error of the calculation. On this basis all iron is thought to be ferrous. Most of the decreased stability of ferrotremolite compared with other ferrous amphiboles is attributable to the vacant *A* site (Ernst, 1968). The decreased linking caused by the ferrous irons also adds to the comparative instability of this amphibole. Riebeckite, which also has a vacant *A* site, is slightly more stable, probably because of the two ferric irons in *M*(2).

The riebeckite-arfvedsonite synthesized by Ernst (1962) on the bulk composition riebeckite comes close to ferrotremolite in stability. Some vacancy in the *A* site as well as some local charge imbalance would account for its lowered stability.

Acknowledgments

The author would like to thank Drs. David R. Wones, Hatten S. Yoder, Jr., David Virgo, and Larry W. Finger for their many comments and suggestions aiding in this study. A special thanks goes to Dr. Hatten S. Yoder, Jr., for arranging monetary support at the Geophysical Laboratory, Carnegie Institution of Washington, and the use of his laboratory equipment there. Dr. David Virgo aided greatly in the Mössbauer interpretations, which are still in progress. Also, I wish to thank Miss Dolores M. Thomas and Mrs. Evelyn Gower for their careful help in preparation of the manuscript.

This investigation was supported by National Science Foundation grants GA1109 and GA13092 to Dr. David R. Wones and by the Geophysical Laboratory.

References

BANCROFT, G. M., AND R. G. BURNS (1969) Mössbauer and absorption spectral study of alkali amphiboles. *Mineral. Soc. Am. Spec. Pap.* **2,** 137–148.

BURNS, R. G., AND F. J. PRENTICE (1968) Distribution of iron cations in the crocodolite structure. *Am. Mineral.* **53,** 770–776.

CAMERON, M., AND G. V. GIBBS (1971) Refinement of the crystal structure of two synthetic fluor-richterites. *Carnegie Inst. Washington Year Book,* **70,** 150–153.

CHARLES, R. W., D. A. HEWITT, AND D. R. WONES (1971) H_2O in lunar processes: The stability of hydrous phases in lunar samples 10058 and 12013. *Proc. Second Lunar Sci. Conf., Geochim. Cosmochim. Acta, Suppl.* **2,** *Vol.* **1,** 645–664.

COLVILLE, P. A., W. G. ERNST, AND M. C. GILBERT (1966) Relationships between cell parameters and chemical compositions of monoclinic amphiboles. *Am. Mineral.* **51,** 1727–1754.

COMEFORO, J. E., AND J. A. KOHN (1955) Synthetic asbestos investigations, II: X-ray and other data on synthetic fluor-richterite, -edenite, and -boron edenite. *Am. Mineral.* **40,** 410–421.

DEER, W. A., R. A. HOWIE, AND J. ZUSSMAN (1963) *Rock Forming Minerals. Vol. 2, Chain Silicates.* John Wiley and Sons, Inc., New York.

DOUGLAS, J. A. V., AND A. G. PLANT (1968) Amphibole: First occurrence in an enstatite chondrite (abstr.). *31st Annu. Meet. Meteorolog. Soc., Cambridge, Mass.*

EITEL, W. (1954) Synthesis of fluorosilicates of the mica and amphibole group. *Proc. Int. Symp. Reactiv. Solids, Gothenburg, 1952,* pp. 335–347.

ERNST, W. G. (1962) Synthesis, stability relations, and occurrence of riebeckite and riebeckite-arfvedsonite solid solutions. *J. Geol.* **70,** 689–736.

——— (1966) Synthesis and stability relations of ferrotremolite. *Am. J. Sci.* **264,** 37–65.

——— (1968) *Amphiboles.* Springer Verlag, New York.

EUGSTER, H. P. (1957) Heterogeneous reactions involving oxidation and reduction at high pressures and temperatures. *J. Chem. Phys.* **26,** 1760–1761.

———, AND G. B. SKIPPEN (1967) Igneous and metamorphic reactions involving gas equilibria. In, P. H. Abelson, Ed., *Researches in Geochemistry, Vol. 2,* John Wiley and Sons, Inc., pp. 492–520.

EVANS, H. T., JR., D. E. APPLEMAN, AND D. S. HANDWERKER (1963) The least squares refinement of crystal unit cells with powder diffraction data by an automatic computer indexing method (abstr.). *Am. Crystallogr. Assoc., Cambridge, Mass., Annu. Meet. Progr.,* pp. 42–43.

FORBES, W. C. (1971) Synthesis and stability relations of richterite. *Am. Mineral.* **56,** 997–1004.

GAY, P., G. M. BANCROFT, AND M. G. BOWN (1970) Diffraction and Mössbauer studies of minerals from

lunar soils and rocks. *Proc. Apollo 11 Lunar Sci. Conf., Geochim. Cosmochim. Acta, Suppl.* **1**, *Vol.* **1**, 481–497.

GHOSE, S. (1966) A scheme of cation distribution in amphiboles. *Mineral. Mag.* **35**, 46–54.

GIBBS, G. V., J. L. MILLER, AND H. R. SHELL (1962) Synthetic fluor-magnesio-richterite. *Am. Mineral.* **47**, 75–82.

GILBERT, M. C. (1966) Synthesis and stability relations of the hornblende ferropargasite. *Am. J. Sci.* **264**, 698–742.

HUEBNER, J. S., AND J. J. PAPIKE (1970) Synthesis and crystal chemistry of sodium-potassium richterite, $(Na,K)NaCaMg_5Si_8O_{22}(OH,F)_2$: A model for amphiboles. *Am. Mineral.* **55**, 1973–1992.

IIYAMA, J. T. (1963) Synthese hydrothermale a 750°C, 1000 bars dans le systeme Na_2O-MgO-Al_2O_3-SiO_2-H_2O d'amphiboles orthorhombiques et monocliniques. *C.R. Acad. Sci. Paris,* **256**, 966–967.

MITCHELL, J. T., F. D. BLOSS, AND G. V. GIBBS (1970) A refinement of the structure of actinolite. *Am. Mineral.* **55**, 302–303.

NICHOLLS, J., AND J. S. E. CARMICHAEL (1969) Peralkaline acid liquids: A petrological study. *Contrib. Mineral. Petrol.* **20**, 268–294.

OLSEN, E. (1967) Amphibole: First occurrence in a meteorite. *Science,* **156**, 61–62.

PAPIKE, J. J., M. ROSS, AND J. R. CLARK (1969) Crystal chemical characterization of clinoamphiboles based on five new structure refinements. *Mineral. Soc. Am. Spec. Pap.* **2**, 117–136.

PHILLIPS, R., AND G. ROWBOTHAM (1968) Studies on synthetic alkali amphiboles. In, *Int. Mineral. Assoc. Pap. Proc. 5th General Meet., Cambridge, 1966.* Mineralogical Society, London, pp. 249–254.

SHANNON, R. D., AND C. T. PREWITT (1969) Effective ionic radii in oxides and fluorides. *Acta Crystallogr.* **B25**, 925–927.

SHAW, H. R. (1967) Hydrogen osmosis in hydrothermal experiments. In, P. H. Abelson, Ed., *Researches in Geochemistry, Vol. 2.* John Wiley and Sons, Inc., pp. 521–541.

WHITTAKER, E. J. W. (1949) The structure of Bolivia crocodolite. *Acta Crystallogr.* **2**, 312–317.

——— (1960) The crystal chemistry of the amphiboles. *Acta Crystallogr.* **13**, 291–298.

WILKINS, R. W. T. (1970) Iron-magnesium distribution in the tremolite-actinolite series. *Am. Mineral.* **55**, 1993–1998.

Manuscript received, September 26, 1973; accepted for publication, December 13, 1973.